Molecular-dynamics simulations for the shock Hugoniot meltings of Cu, Pd and Pt

1999 J. Phys.: Condens. Matter 11 3799

(http://iopscience.iop.org/0953-8984/11/19/302)

J. Phys.: Condens. Matter **11** (1999) 3799–3806. Printed in the UK PII: S0953-8984(99)01702-6

Molecular-dynamics simulations for the shock Hugoniot meltings of Cu, Pd and Pt

Ji-Wook Jeong and K J Chang

Department of Physics, Korea Advanced Institute of Science and Technology, Taejon 305-701, Korea

Received 9 February 1999

Abstract. We perform molecular-dynamics simulations to study the shock melting of transition metals such as Cu, Pd and Pt on the basis of an embedded-atom method. Using the coupling-constant integration method, the Gibbs free energies of the crystalline and liquid phases are calculated as a function of pressure and temperature, so that the melting curves are obtained, up to 3–4 Mbar. We find the melting properties near zero pressure to be in good agreement with experiments. For each metal, we compare the melting curve with the Hugoniot equations of state for the solid and liquid phases and determine the melting region of the shock Hugoniot. The Hugoniot melting of Cu is found to begin at 1.9 Mbar and to end at 2.25 Mbar, in good agreement with experimental data. During the shock compression, we find that the pressure region where the Hugoniot melting occurs increases almost linearly with increase of the ionic mass.

1. Introduction

Molecular-dynamics (MD) simulations have been very successful for studying the thermodynamic properties of real materials [1–3]. Since the MD technique provides rich information on the trajectories of ions, it is used as a basic tool for investigating the time evolution of atomic positions, the determination of equilibrium atomic geometries, the direct observation of structural phase transformations, and so on [4–7]. Although there have been several theoretical approaches which do not rely on MD simulations, these calculations required a lattice-dynamics model for the phonon free energy of the solid phase and a suitable reference system for the free energy of the liquid phase [8, 9]. In the MD approach, with use of the thermodynamic integration method, the Gibbs free energies of both the solid and liquid phases can be directly calculated as a function of temperature and pressure, so that the melting temperatures of materials are evaluated very accurately [10–12]. This method avoids the harmonic-crystal approximation and the calculations of the phonon spectrum. Despite remarkable progress on the first-principles description of electron–electron interactions and the computational efficiency, first-principles MD simulations for transition metals are still challenging problems because of the heavy computational demand. In addition, it is not clear whether the density-functional approximation can describe accurately the ground-state properties of transition metals and their high-pressure and high-temperature properties. In view of this, the use of empirical potentials can give insight into the main behaviour which is otherwise difficult to get from first-principles calculations, which are desirable. The melting properties of Al near zero pressure have been studied using MD simulations based on an embedded-atom method (EAM) [13]. In subsequent studies, the same EAM potential for Al was used to calculate the melting curve up to 1.6 Mbar and the solid and liquid Hugoniots [14]. These calculational

0953-8984/99/193799+08$19.50

results demonstrated that the EAM potential is accurate enough to describe both the static and dynamic properties of Al, with high computational efficiency.

In this paper, we perform MD simulations to investigate the melting properties of fcc transition metals such as Cu, Pd and Pt near zero pressure using the embedded-atom method, and find good agreements with experiments. We obtain the melting curves up to 3–4 Mbar and determine the pressure region where the Hugoniot melting occurs. We find that the Hugoniot melting pressure tends to increase with increasing ionic mass.

In section 2 we describe computational methods for the calculations of the Gibbs free energies for the solid and liquid phases and details of the molecular-dynamics simulations. In section 3 the calculated melting curves and Hugoniot equations of state for Cu, Pd and Pt are given and discussed. The results are summarized in section 4.

2. The molecular-dynamics simulation method

The internal energies (U) of the transition metals are calculated using the embedded-atom method, which has been very successful in describing the ground-state properties [8, 13]. We employ the parameters in the EAM potentials which were previously determined to reproduce the measured values for the cohesive energy, equilibrium lattice constant, and elastic constants at normal pressure [13]. The Gibbs free energy at temperature T and pressure P is calculated using the coupling-constant integration method [15], which gives a difference of the Gibbs free energies at two different temperatures. In this case, the Einstein solid with the oscillator strength characterized by the Debye temperature is chosen as a reference system for the solid phase. For the liquid phase, although an ideal-gas system is usually employed as a reference system, an intermediate reference system with only repulsive interactions is required to avoid the possible liquid–gas phase transition [1]. This reference system is obtained by a gradual turning off of the attractive part of U at constant volume $V_0 = V(T_0, P)$, followed by a reversible volume expansion process to infinite volume at a reference temperature T_0. The details of the calculational procedure for the Gibbs free energies are given elsewhere [13, 14].

In molecular-dynamics simulations, we use a Nosé thermostat [16] to control the temperature of the ions, which provides the canonical trajectories for the ionic motions. To perform isobaric molecular-dynamics simulations, we employ the variable-cell-shape technique proposed by Wentzcovitch [17] and co-workers. The equations of motion for the atomic positions, thermostat, and cell edges are integrated simultaneously using the fifth-order predictor–corrector algorithm, with a time step of 10.5 au (=0.254 fs) for the whole temperature range considered here. For each simulation run, we first equilibrate the system for a period of 4000 time steps ($\simeq$1 ps) and integrate an additional 6000 time steps ($\simeq$1.5 ps) to calculate the statistical average for a particular thermodynamic state at P and T. For the solid phase, we start from a simple cubic supercell containing 256 atoms with periodic boundary conditions, initially arranged in a fcc lattice. We use the output configuration of each run as a starting system for the next run. For the liquid phase, we start from a completely melted configuration at very high temperature to avoid the superheated state in the simulation of isobaric heating. The reference temperatures for the solid and liquid phases are chosen to be close to the thermodynamic melting temperature, so that the accumulated errors in the Gibbs free energy are eliminated.

We obtain the melting point at a given pressure by finding the equal Gibbs free energies of the solid and liquid phases, and extend molecular-dynamics simulations to the pressure regime 3–4 Mbar to determine the melting curve. Considering a wide range of temperature and pressure, we obtain the isothermal equations of state for various temperatures and construct the Hugoniot equation of state which satisfies the Rankine–Hugoniot relation. The solid

Hugoniot curve is obtained for pressures up to 4.0 Mbar, while for the liquid phase the pressure is increased to 5.5 Mbar. Thus, we determine the pressure region where the Hugoniot melting occurs, by comparing the melting curve with the Hugoniot equation of state for each phase.

3. Results and discussion

First we examine the static structure factor $S(q)$ of liquid Cu, which is generated at 1500 K through molecular-dynamics simulations. We find that the EAM potential well reproduces the peak structure of $S(q)$ [18], as shown in figure 1. Then, we perform the thermodynamic integrations to obtain the Gibbs free energies for a wide range of temperature and pressure. In this case, the reference temperatures for the solid and liquid phases at zero pressure are set to be $T_0 = 1200$ and 1500 K, respectively. The Gibbs free energy of solid Cu at 1200 K is calculated to be -4.02 eV/atom, as compared to the measured value of -4.06 eV/atom [19], whereas for the liquid phase the Gibbs free energy is -4.28 eV/atom at 1500 K. By finding the equal Gibbs free energies of the solid and liquid phases, we estimate the melting temperature (T_m) to be 1246 K, similar to the previous EAM results of 1340 and 1171 K [8, 20]. Our calculated melting temperature is lower by about 110 K than the experimentally measured value of 1357 K [19], indicating that the calculational accuracy for T_m is comparable to that for Al [2, 14]. The results for the zero-pressure thermodynamic quantities at the melting point are listed and compared with other calculations and experiments in table 1. The volume change during the melting transition is estimated to be 0.81 Å^3/atom, while the measured

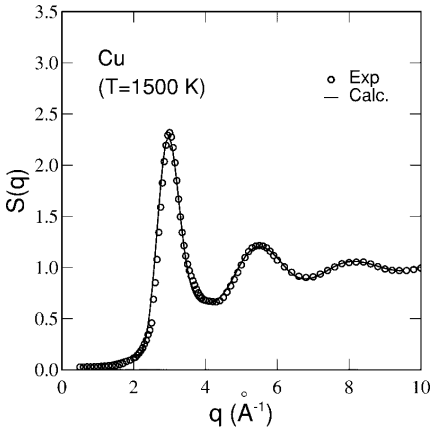

Figure 1. The calculated static structure factor $S(q)$ (solid curve) of liquid Cu at 1500 K is compared with experimental data (circles) from reference [18].

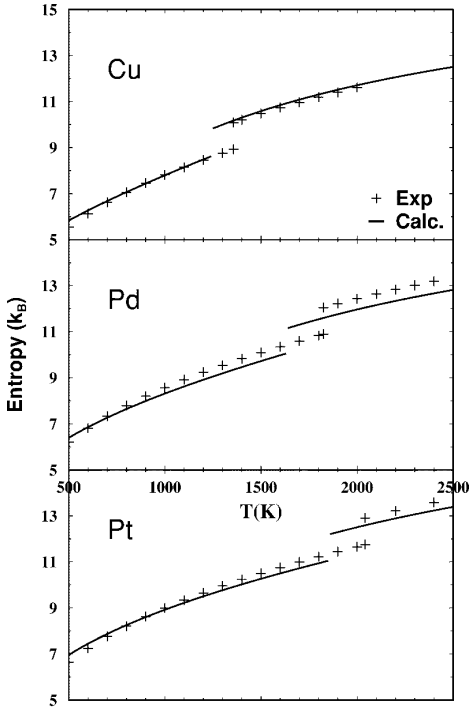

Figure 2. The calculated entropies (solid curves) for the solid and liquid phases of Cu, Pd and Pt are compared with experimental data (crosses) from reference [19].

Table 1. The zero-pressure melting properties of Cu, Pd and Pt are compared with experiments. Here T_m, ΔS_m, ΔV_m and L denote the melting point, entropy change, volume change and latent heat at T_m.

		T_m (K)	ΔV_m (Å^3/atom)	ΔS_m (k_B)	L (eV/atom)	$\mathrm{d}P_m/\mathrm{d}T_m$ (kbar K^{-1})
Cu	Experiment	1358[a]	0.52[b]	1.16[a]	0.14[a]	0.2381[b]
	Other EAM	1340[c], 1171[d]				
	Our EAM	1246	0.81	1.18	0.13	0.20
Pd	Experiment	1828[a]		1.107[a]	0.17[a]	
	Other EAM	1390[c], 1520[e], 1828[e]				
	Our EAM	1635	0.76	1.08	0.15	0.20
Pt	Experiment	2042[a]	0.60[b]	1.159[a]	0.23[a]	0.20[b]
	Other EAM	1480[c]				
	Our EAM	1853	0.78	1.14	0.18	0.20

[a] Reference [19].
[b] Reference [21].
[c] Reference [8].
[d] Reference [20].
[e] Reference [27].

value is 0.52 Å^3/atom [21]. The calculated entropies of the solid and liquid phases are found to be in good agreement with experiments [19], as shown in figure 2, while in previous EAM calculations they are slightly overestimated for Al [14]. From the change of entropy, the latent heat of transformation is calculated to be about 0.13 eV/atom, very close to the measured value of 0.14 eV/atom [19]. Using the melting properties near zero pressure, we estimate an initial slope of the melting temperature with respect to pressure, i.e., $\mathrm{d}P_m/\mathrm{d}T_m = 0.20$ kbar K^{-1},

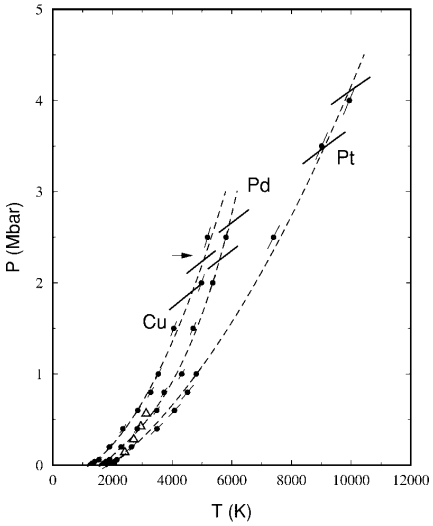

Figure 3. The melting curves (dashed curves) for Cu, Pd and Pt are shown. The thick solid line segments represent the Hugoniot meltings for the solid and liquid phases, while experimental data (reference [28]) for Pt are denoted by triangles. The small line segments through the solid circles represent the slopes $\mathrm{d}P_m/\mathrm{d}T_m$ determined from the Clausius–Clapeyron equation. The arrow indicates the measured value (reference [22]) for Cu.

which is obtained from the thermodynamic relation known as the Clausius–Clapeyron equation ($dP_m/dT_m = \Delta S_m/\Delta V_m$), close to the experimental value of 0.24 kbar K^{-1} [21].

To find the melting curve in the high-pressure region, we perform molecular-dynamics simulations for eight different pressures between 0 and 2.5 Mbar. For each pressure, the melting point is determined by the equal-free-energy condition. Combining this with the calculational results for low pressures, below 0.06 Mbar, we obtain the melting curve which is well represented by a parabolic fitting, as illustrated in figure 3. We find the pressure variation of the melting temperature near zero pressure to be $dP_m/dT_m = 0.20$ kbar K^{-1}, in good agreement with the results obtained from both the Clausius–Clapeyron equation and experiments [21]. To obtain the shock Hugoniot of Cu, we first calculate the isotherms for several selected pressures up to 3 Mbar. To determine the melting pressures on the shock Hugoniot, we combine the melting curve and the Hugoniot equations of state for the solid and liquid phases. We find that the Hugoniot melting begins at about 1.9 Mbar and ends at 2.25 Mbar, as shown in figure 3, consistent with the experimentally measured value of 2.3 Mbar [22]. During the Hugoniot process, the calculated atomic densities are found to be larger by about 3% than the measured values [23–25], as shown in figure 4(a). The calculated Hugoniot temperature determined from the Rankine–Hugoniot relation rises as high as 3200 K at 1.5 Mbar, while experimentally it was suggested to be about 3000 K, on the basis of the Mie–Grüneisen equation of state [26]. The shock-wave velocity shows a linear relationship with the mass velocity, which was also observed in shock-wave experiments [23]; however, its slope is slightly larger than the measured value because of the overestimation of the densities (see figure 4(b)).

Next we investigate the melting properties of Pd, which is heavier by about 67% than Cu.

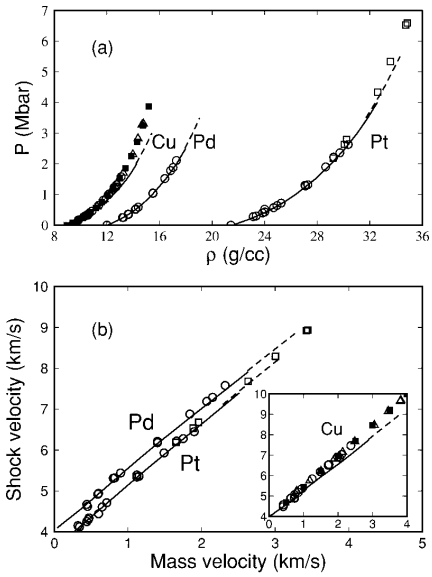

Figure 4. (a) The calculated Hugoniot equations of state for Cu, Pd and Pt are compared with the results from shock experiments. (b) The shock-wave velocities are plotted as a function of mass velocity for Pd and Pt, while the results for Cu are given in the inset. Solid and dashed lines represent the calculational results for the solid and liquid phases, respectively. Experimental data are represented by circles (reference [25]), triangles (reference [23]), solid boxes (reference [24]) and empty boxes (reference [30]).

The reference temperatures (T_0) for the solid and liquid phases at zero pressure are chosen to be 1000 and 2500 K, respectively. The Gibbs free energy of solid Pd at 1000 K is calculated to be -4.33 eV/atom, in good agreement with the measured value of -4.37 eV/atom [19], while for the liquid phase the Gibbs free energy is found to be -5.74 eV/atom at $T_0 = 2500$ K. The melting temperature at zero pressure is estimated to be 1635 K, which is higher than that for Cu. This calculated value for T_m is underestimated by about 190 K compared with the measured value of 1828 K [19], while in other EAM calculations lower melting temperatures of 1390 and 1520 K were obtained [8, 27]. In table 1, various thermodynamic quantities at the melting point are summarized. During the melting transition, the volume of the liquid phase is found to be expanded by 0.76 Å^3/atom. The temperature variations of the entropy for both the solid and the liquid phases are shown in figure 2, and the latent heat of transformation estimated from the change of entropy is about 0.15 eV/atom, in good agreement with the experimental value of 0.14 eV/atom [19]. From the Clausius–Clapeyron equation, we estimate the initial slope of the melting temperature with respect to pressure to be $\mathrm{d}P_m/\mathrm{d}T_m = 0.20$ kbar K^{-1}, similar to the result for Cu.

The melting temperatures for 11 different pressures up to 2.5 Mbar are plotted in figure 3. From the melting curve, the initial pressure variation of the melting temperature is found to be $\mathrm{d}P_m/\mathrm{d}T_m = 0.23$ kbar K^{-1}, and this value is close to the result estimated from the Clausius–Clapeyron equation at zero pressure. We find the Hugoniot melting to begin at about 2.25 Mbar and to end at 2.65 Mbar. The calculated atomic densities during the shock compression are found to be in good agreement with experiments [25], as shown in figure 4(a). From the Rankine–Hugoniot relation, the Hugoniot temperature is increased up to 4600 K at 2.0 Mbar. We find a linear relationship between the shock and mass velocities in the Hugoniot process, as shown in figure 4(b), and the results are in good agreement with experiments.

For Pt, we choose the reference temperatures for the solid and liquid phases to be $T_0 = 1000$ and 2500 K, respectively. The Gibbs free energy of solid Pt at zero pressure is calculated to be -6.34 eV/atom at 1000 K, consistent with the measured value of -6.35 eV/atom [19]. For the liquid phase, the Gibbs free energy is found to be -7.79 eV/atom at $T_0 = 2500$ K. The melting temperature at zero pressure is calculated to be 1853 K, and this value is lower by about 190 K than the experimental value of 2042 K [19]. The calculated volume change during the solid–liquid melting transition is 0.78 Å^3/atom (see table 1), while the measured value is 0.60 Å^3/atom [21]. For both the solid and liquid phases, the calculated entropies are in good agreement with experiments [19], as shown in figure 2. Near zero pressure, we find a latent heat of about 0.18 eV/atom and the slope of the melting temperature with respect to pressure to be $\mathrm{d}P_m/\mathrm{d}T_m = 0.20$ kbar K^{-1}, while the corresponding measured values are 0.23 eV/atom and 0.20 kbar K^{-1}, respectively [19, 21].

To determine the melting curve, we perform molecular-dynamics simulations for pressures up to 4 Mbar. The pressure variation of the melting temperature near zero pressure is found to be $\mathrm{d}P_m/\mathrm{d}T_m = 0.20$ kbar K^{-1}, consistent with the results from the Clausius–Clapeyron equation and experiments [21]. Our calculated melting curve is compared with recent experimental results in figure 3, which were obtained using a laser-heated diamond cell up to 0.7 Mbar [28]. We find that the measured variation of the melting point with increasing pressure is slower than that indicated by our calculations, i.e., giving a larger value of $\mathrm{d}P_m/\mathrm{d}T_m = 0.37$ kbar K^{-1}. At this point, it is not clear what causes the discrepancy between the calculated and measured melting curves. Here we point out that the melting curve is sensitive to the statistical analysis of the melting data; for example, three independent static measurements for Al were shown to give different melting slopes [29]. To obtain the Hugoniot equation of state, we generate the isotherms for pressures up to 5.5 Mbar. From the melting curve and the two sets of Hugoniot data for the solid and liquid phases, the pressure region of the shock melting is found to lie

between 3.5 and 4.1 Mbar, as shown in figure 3. We find the temperature of liquid Pt to be as high as 16 800 K at 5.5 Mbar. In the Hugoniot process, the relation between the shock-compressed atomic density and pressure as well as the shock–mass-velocity relation are in good agreement with experimental data [25, 30], as illustrated in figure 4.

We find that the EAM potentials used here generally underestimate the melting temperatures of fcc transition metals such as Cu, Pd and Pt by 100–200 K at normal pressure, compared with experimental data. A similar underestimation of the melting point was also found for Al [14]. The initial slopes of the melting temperatures with respect to pressure, which are obtained from the melting properties near zero pressure, are found to be consistent with those directly calculated from the melting curves, confirming the self-consistency of our calculations. These slopes are also in good agreement with the measured values, except for Pt, where the melting data from laser-heated cell experiments up to 0.7 Mbar show a larger slope for $\mathrm{d}P_m/\mathrm{d}T_m$. However, for both the solid and liquid phases of Pt, our calculational results for the Hugoniot equations of state and the relation between the shock and mass velocities are in good agreement with experiments. To resolve the discrepancy between the calculated and measured values for $\mathrm{d}P_m/\mathrm{d}T_m$ for Pt, further experimental studies are needed. On the basis of our results, we note that the pressure region where the Hugoniot melting occurs generally increases with increasing ionic mass, as shown in figure 5. Thus, our calculations demonstrate that although the parameters in the EAM potential are determined to generate the ground-state properties at normal pressure, the EAM potential describes the dynamic properties of the fcc transition metals considered here reasonably well.

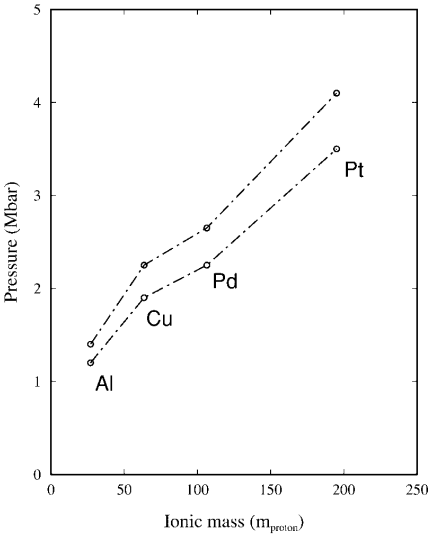

Figure 5. The pressure region where the Hugoniot melting occurs is plotted as a function of ionic mass. The results for Al are from reference [14].

Finally, we discuss the accuracy of the EAM potential in molecular-dynamics simulations at very high temperatures. For liquid Cu, Pd and Pt, we find good agreements between the calculated and measured structure factors, indicating that the liquid phase is well generated by molecular-dynamics simulations. Among the transition metals considered here, Pd has the highest density of states at the Fermi level because of the filled d shell. In this case, the electronic contribution to the Gibbs free energy at very high temperature, where electrons are excited above the Fermi level, may not be negligible. Since this contribution may decrease the melting temperature, it is desirable to perform first-principles molecular-dynamics simulations, if possible.

4. Summary

In summary, we have calculated the melting curves up to 3–4 Mbar for Cu, Pd and Pt through molecular-dynamics simulations based on the embedded-atom method. The melting properties near zero pressure are in good agreement with both previous theoretical calculations and experiments. However, we find a discrepancy between the calculated melting curve and that obtained from melting data up to 0.7 Mbar for Pt; further studies are required to resolve such a discrepancy. We find the solid and liquid Hugoniots to be in good agreement with experimental shock data. On the basis of the results for the melting curves and the Hugoniot equations of state, we have determined the melting region where the Hugoniot melting occurs.

Acknowledgments

This work was supported by the ADD, the MOST-FOTD project and the CMS at KAIST.

References

[1] Broughton J Q and Li X P 1987 *Phys. Rev.* B **35** 9120
[2] Mei J and Davenport J W 1992 *Phys. Rev.* B **46** 21
[3] Wentzcovitch R M 1994 *Phys. Rev.* B **50** 10 358
Bernasconi M, Chiarotti G, Focher P, Scandolo S, Tosatti E and Parrinello M 1995 *J. Phys. Chem. Solids* **56** 501
[4] Zhang B L, Xu C H, Wang C Z, Chan C T and Ho K M 1992 *Phys. Rev.* B **46** 7333
[5] Wentzcovitch R M, Martins J L and Price G D 1993 *Phys. Rev. Lett.* **70** 3947
[6] Wentzcovitch R M 1994 *Phys. Rev.* B **50** 10 358
[7] Scandolo S, Bernasconi M, Chiarotti G L, Focher P and Tosatti E 1995 *Phys. Rev. Lett.* **74** 4015
[8] Foiles S M and Adams J B 1989 *Phys. Rev.* B **40** 5909
[9] Moriarty J A, Young D A and Ross M 1984 *Phys. Rev.* B **30** 578
[10] Sugino O and Car R 1995 *Phys. Rev. Lett.* **74** 1823
[11] Gu Y M, Bylander D M and Kleinman L 1995 *Phys. Rev.* B **51** 15 703
[12] de Wijs G A, Kresse G and Gillan M J 1998 *Phys. Rev.* B **57** 8223
[13] Mei J, Davenport J W and Fernando G W 1991 *Phys. Rev.* B **43** 4653
[14] Jeong J W, Lee I H, Oh J H and Chang K J 1999 *Phys. Rev.* B **59** 329
[15] Ciccotti G and Hoover W G (ed) 1986 *Molecular-Dynamics Simulation of Statistical-Mechanical Systems* (Amsterdam: North-Holland) pp 169–78
[16] Nosé S 1986 *Mol. Phys.* **57** 187
[17] Wentzcovitch R M 1991 *Phys. Rev.* B **44** 2358
[18] Waseda Y 1980 *The Structure of Non-Crystalline Materials* (New York: McGraw-Hill)
[19] Hultgren R, Desai P D, Hawkins D T, Gleiser M, Kelley K K and Wagman D D 1973 *Selected Values of the Thermodynamic Properties of Binary Alloys* (Metals Park, OH: American Society for Metals)
[20] Lutsko J F, Wolf D, Phillpot S R and Yip S 1989 *Phys. Rev.* B **40** 2841
[21] Paul W and Warschauer D M (ed) 1963 *Solids under Pressure* (New York: McGraw-Hill) p 314
[22] Nellis W J, Moriarty J A, Mitchell A C, Ross M, Dandrea R G, Ashcroft N W, Holmes N C and Gathers G R 1988 *Phys. Rev. Lett.* **60** 1414
[23] Mitchell A C and Nellis W J 1979 *J. Appl. Phys.* **52** 3363
[24] Al'tshuler L V, Kormer S B, Bakanova A A and Trunin R F 1960 *Sov. Phys.–JETP* **11** 573
[25] Kinslow R (ed) 1970 *High-Velocity Impact Phenomena* (New York: Academic) pp 515–23
[26] McQueen R G and Marsh S P 1960 *J. Appl. Phys.* **31** 1253
[27] Wolf R J, Mansour K A, Lee M W and Ray J R 1992 *Phys. Rev.* B **46** 8027
[28] Kavner A and Jeanloz R 1998 *J. Appl. Phys.* **83** 7553
[29] Lees J and Williamson B H J 1965 *Nature* **208** 278
[30] Holmes N C, Moriarty J A, Gathers G R and Nellis W J 1989 *J. Appl. Phys.* **66** 2962